Proc. Natl. Acad. Sci. USA
Vol. 80, pp. 5281–5285, September 1983
Biochemistry

Monoclonal antibodies to rat Na^+,K^+-ATPase block enzymatic activity

(mouse hybridoma/sodium pump/enzyme inhibition/immunofluorescence)

DALE B. SCHENK AND HYAM L. LEFFERT*

Department of Medicine, Division of Pharmacology, M-013 H, University of California at San Diego, La Jolla, California 92093

Communicated by Morris Friedkin, June 6, 1983

ABSTRACT **A panel of nine mouse monoclonal antibodies has been prepared against purified preparations of rat kidney Na^+,K^+-ATPase (EC 3.6.1.3). Selection for specific antibody was based upon the ability of crude hybridoma fluids to inhibit Na^+-ATPase activity (using luciferase-linked ATPase assays) and upon antibody binding to both the purified kidney membrane enzyme and to glutaraldehyde-fixed hepatocytes by using standard enzyme-linked immunoadsorbent assays. After immunoaffinity purification, two of the antibodies (both of the IgG1 subclass) fully inhibit kidney and liver membrane Na^+,K^+-ATPase activity with K_i (apparent) values of 30 nM ("9-A5") and 600 nM ("9-B1"). Immunoblots demonstrate directly that three different ^{125}I-labeled antibodies (6-4, 9-A5, and 9-B1) bind predominantly to a 94,000 M_r protein that comigrates in $NaDodSO_4$/polyacrylamide gels with the fluorescein isothiocyanate-labeled α subunit of the Na^+,K^+-ATPase. Indirect immunofluorescence studies with these antibodies on paraformaldehyde-fixed liver slices reveal staining patterns congruent with bile canalicular membrane domains. These results together suggest that the antibodies exert inhibitory effects by recognizing α subunits of both liver and kidney Na^+ pumps in their native conformations.**

Mitogen-activated Na^+ influxes across the plasma membrane are implicated in the initiation of animal cell proliferation (1). These fluxes are linked to several "early" prereplicative amiloride-sensitive events, including: (*i*) accelerated ouabain-sensitive $^{86}Rb^+$ uptake; (*ii*) accelerated Na^+/H^+ and Na^+/Ca^{2+} exchange; (*iii*) membrane potential depolarization; (*iv*) increases in rates of Na^+-dependent amino acid cotransport; (*v*) increases in nuclear Na^+ content; and (*vi*) alterations in protein phosphorylation. Despite these and other related findings, none has shown strict causal relationships to DNA synthesis initiation late in the prereplicative phase (reviewed in ref. 2).

One reason for this uncertainty is that drugs that block membrane cation fluxes and prolong DNA synthesis onset times (1–5), such as amiloride (a passive Na^+-influx inhibitor) or ouabain (a Na^+,K^+-ATPase inhibitor), concentrate inside cells (6, 7) and exert nonspecific side effects (7, 8). In an attempt to avoid the latter problem, we have begun to develop monoclonal antibodies against cell surface ion transporting structures whose functions are blocked by these drugs. In this report, we describe the characterization of a panel of such antibodies that bind to and inhibit enzyme activity of the ouabain-sensitive Na^+ pump. Preliminary accounts of these results were reported elsewhere (3, 9).

MATERIALS AND METHODS

Purification of Rat Na^+,K^+-ATPase. Purified Na^+,K^+-ATPase was prepared from outer renal medullas of male Sprague–Dawley rats (300–500 g; Charles River Breeding Laboratories) by standard procedures (10). Preparations were examined by $NaDodSO_4$/polyacrylamide gel electrophoresis and judged >75% pure by densitometric scanning at 540 nm of Coomassie blue-stained gels. Specific activities of the preparations were 6–15 μmol of P_i released per mg of protein per min, as determined by NADH-coupled enzyme assays (11). Crude liver membranes were prepared by Neville's method (12).

Hybridoma Production. Male 10–20 g BALB/c mice (Charles River Breeding Laboratories) were immunized intramuscularly in the hindleg with 10 μg of purified rat Na^+,K^+-ATPase in complete Freund adjuvant. At 3 wk, booster injections of incomplete Freund adjuvant containing 10 μg of antigen proteins were made at identical sites. Antisera were titered 1 wk later by using enzyme-linked immunoadsorbent assays (ELISAs) (13). Mice with high titers [A_{490} values >2× background (see Fig. 1) with antisera dilutions ≥1:50,000] were injected intraperitoneally with 10 μg of antigen, and 4 days later their spleens were obtained.

Cell fusions were performed by standard procedures (14). The parental mouse myeloma NS-1/1.Ag 4.1 was obtained from S. Sell (University of Texas, Houston, TX). Hybridoma colonies were screened for specific antibody production by ELISA (described below) and by inhibition of Na^+-ATPase activity (15). Colonies generating "positive" media were propagated, frozen, and cloned in soft agar at least twice to ensure stable antibody production (16). The nine hybridoma lines reported here have been grown for >100 generations without detectable changes in antibody production.

ELISA. Two different microtiter plate assays were developed and characterized according to standard procedures (13): (*i*) using antigen coatings of 0.5 μg of purified rat kidney Na^+,K^+-ATPase proteins per well ("antigen" ELISA) and (*ii*) using antigen coatings of primary cultures of 1-day-old adult rat hepatocytes (5×10^4 cells plated per well; ref. 1), washed with phosphate-buffered saline (P_i/NaCl) (pH 7.4), and fixed with 1% (wt/vol) glutaraldehyde ("hepatocyte" ELISA). Fluids containing primary antibody (antisera, hybridoma media, or purified monoclonal antibodies) were diluted serially 1:5 in 100 μl of P_i/NaCl per well and incubated 2 hr at 37°C. After washing four times with 200 μl of P_i/NaCl at 21°C, 100 μl of 1:3,000 dilutions of rabbit anti-mouse (IgG and IgM) horseradish peroxidase conjugate antiserum per well (Boehringer Mannheim) was incubated 2 hr at 37°C. Two hundred microliters of *o*-phenylenediamine (0.3 mg/ml, Sigma) was added to each well. Product formation was monitored after 30 min at 21°C by increases in A_{490}. Half-maximal A_{490} values were calculated from

The publication costs of this article were defrayed in part by page charge payment. This article must therefore be hereby marked "*advertisement*" in accordance with 18 U.S.C. §1734 solely to indicate this fact.

Abbreviations: ELISA, enzyme-linked immunoadsorbent assay; P_i/NaCl, phosphate-buffered saline; $C_{12}E_8$, octaethylene glycododecyl ether; FITC, fluorescein isothiocyanate; TRITC, trimethyl rhodamine isothiocyanate.

* To whom reprint requests should be addressed.

purified monoclonal antibody titers (ng per well) required to produce 50% of maximal absorbance.

ATPase Activity Determinations. Luciferase-linked Na^+-ATPase assays, used to screen for inhibitory hybridoma media, employed 1 μM ATP, 100 mM NaCl, and 5 mM $MgSO_4$ in the absence of KCl (15). Standard P_i-release (17) or NADH-coupled enzyme assays were used to quantitate Na^+,K^+-ATPase activity under V_{max} conditions (3 mM ATP, 100 mM NaCl, 20 mM KCl, and 5 mM $MgCl_2$) at 30°C. In some assays (as noted) purified rat Na^+,K^+-ATPase was solubilized in octaethylene glycododecyl ether ($C_{12}E_8$; Nikko Chemicals, Tokyo) with detergent/protein ratios adjusted to 2.5:1.0 (18).

The percentage of ouabain-sensitive ATPase activity was calculated as the fraction of ouabain-sensitive ATPase activity remaining after addition of antibody × 100.

Antibody Purification. Monoclonal antibodies were purified by immunoaffinity chromatography over rabbit anti-mouse (IgG, IgM, and IgA) (Cappel Laboratories, Cochranville, PA) coupled to CNBr-activated Sepharose 4B (Pharmacia) (3 mg of rabbit Ig per ml of packed gel). Bound antibody was eluted with 0.1 M glycine (pH 2.8), neutralized with NaOH to pH 7.0, dialyzed against distilled H_2O for 48 hr, and lyophilized. Purified antibodies were reconstituted with 0.15 M NaCl and protein concentrations were determined (19).

Ouchterlony Double-Immunodiffusion. Characterization of monoclonal antibody immunoglobulin subclass was performed with subclass-specific goat anti-mouse IgG (Meloy, Springfield, MI) (20).

Immunoblots. Purified rat Na^+,K^+-ATPase (200–500 μg of proteins per gel) and pure protein markers (Bio-Rad) were electrophoresed on 10% polyacrylamide slab gels. One gel track contained enzyme preparations specifically labeled with fluorescein isothiocyanate (FITC) to localize Na^+,K^+-ATPase α subunits (21). Standard procedures were used to electrophoretically transfer proteins from $NaDodSO_4$ gels onto nitrocellulose paper (22). After protein transfer, 7.5-mm strips were incubated with 1×10^6 cpm of ^{125}I-labeled monoclonal antibody per ml for 2 hr at 4°C in blot buffer [20 mM Tris (base)/100 mM NaCl/1% (wt/vol) bovine serum albumin/0.2% Nonidet P-40, pH 7.5]. The strips were washed with blot buffer four times (10-min intervals at 4°C), dried, and subjected to autoradiography. FITC-labeled α subunits were visualized by UV fluorescence.

Radiolabeling and Autoradiography. Purified monoclonal antibodies were iodinated by using lactoperoxidase, glucose oxidase, and $Na^{125}I$ (23). ^{125}I-Labeled antibodies were separated from free iodine by Sephadex G-100 chromatography and their integrity was verified by $NaDodSO_4$/polyacrylamide gel electrophoresis and autoradiography. Samples (specific activity, 8–10 μCi/μg of protein; 1 Ci = 3.7×10^{10} Bq) were stable for 3–4 wk as aliquots at −70°C. Autoradiography was performed with Kodak XRP-1 film and Kodak X-Omat intensifying screens for 1–7 days at −70°C.

$NaDodSO_4$/Polyacrylamide Gel Electrophoresis. Discontinuous $NaDodSO_4$/polyacrylamide gel electrophoresis was performed under denaturing conditions according to Laemmli (24). The stacking and running gels were 2% and 10% (wt/vol) acrylamide, respectively. Gels were stained with either Coomassie brilliant blue or $AgNO_3$ (25).

Immunofluorescence. Male 200–300 g Fisher/344 rats (Charles River Breeding Laboratories) were anesthetized with ether. Perfusions through abdominal aortic canulae were performed at 21°C with 125 ml of Ringer solution, followed by 125 ml of paraformaldehyde/lysine/periodic acid fixative (26). Liver pieces were excised, embedded in agar, and cut into 20-μm sections by using a Lerner Vibrotome at 4°C. All subsequent incubations were performed at 4°C on a rotary shaker. Thin sections were blocked for nonspecific binding with 1:40 dilutions of normal goat serum for 10 min. The sections were washed two times in P_i/NaCl (15 min each) and incubated with 100 μg of purified antibody per ml for 16 hr. After three 10-min washes with P_i/NaCl, the sections were incubated with 0.1–0.4 mg of trimethyl rhodamine isothiocyanate (TRITC)-labeled goat anti-mouse IgG per ml (Cappel Laboratories) for 30 min, washed four times in P_i/NaCl (5 min each), and mounted on coverslips in glycerol. Fluorescence microscopy was performed with an inverted Nikon DIAPHOT-TMD microscope, equipped with an epi-fluorescence attachment (λ_{excit} = 546 nm; λ_{emit} = 580 nm), ×40 fluorite lens, and mercury lamp. Photomicrographs were taken on 35-mm Kodak film (ASA 400) by using a Nikon Micro-HFX attachment.

RESULTS

Molecular Properties. Purified antibodies were analyzed by $NaDodSO_4$/polyacrylamide gel electrophoresis and immunodiffusion in agar to determine subunit M_r and heavy chain Ig subclasses, respectively (Table 1). Except for 6-6 and 12-3, no two antibodies were alike by these criteria. As expected (16), discrete heavy to light chain ratios (1:1, 2:1, and 1:2) were observed. Of the four subclasses found, IgG1 predominated. However, no antibody reacted with more than one subclass-specific goat antiserum, as expected for hybridoma clones producing a single antibody.

Table 1. Characterization of purified mouse monoclonal anti-rat Na^+,K^+-ATPase antibodies

Hybridoma clone	Ig subclass	$M_r \times 10^{-3}$* Light chain	$M_r \times 10^{-3}$* Heavy chain	Recognition site†	ELISA binding,‡ ng at half-maximal A_{490}	Enzymatic effects Na^+,K^+-ATPase	Enzymatic effects Na^+-ATPase§
6-2	IgM	28	72	NT	1,500 (K); 300 (H)	0	0
6-4	IgG2A	25, 27	72	α	5,000 (K); 50 (H)	0	0
6-6	IgM	26, 29	75	α	400 (K); 500 (H)	0	–
6-8	IgG2B	25, 29	57	α	5,000 (K); 1,000 (H)	0	–
7-C	IgM	27, 29	66, 75	NT	10,000 (K); 1,000 (H)	0	–
9-A5	IgG1	31	55	α	5,000 (K); 2,000 (H)	–	–
9-B1	IgG1	25, 28	53	α	80 (K); 1,000 (H)	–	–
9-B3	IgG1	26	52, 56	NT	80 (K); 1,000 (H)	0	0
12-3	IgM	26, 28	72	NT	400 (K); 2,000 (H)	0	0

Unless noted, antibodies were obtained from media harvested from stationary-phase cell cultures and were affinity purified. NT, not tested; K, kidney membrane antigens; H, fixed hepatocytes; − = inhibition; 0 = no effect.

* Determined from $NaDodSO_4$/polyacrylamide gel electrophoresis.

† Determined from immunoblot and autoradiography.

‡ Determined from ELISAs.

§ Hybridoma media (200 μl/1-ml assay tube, described in ref. 15).

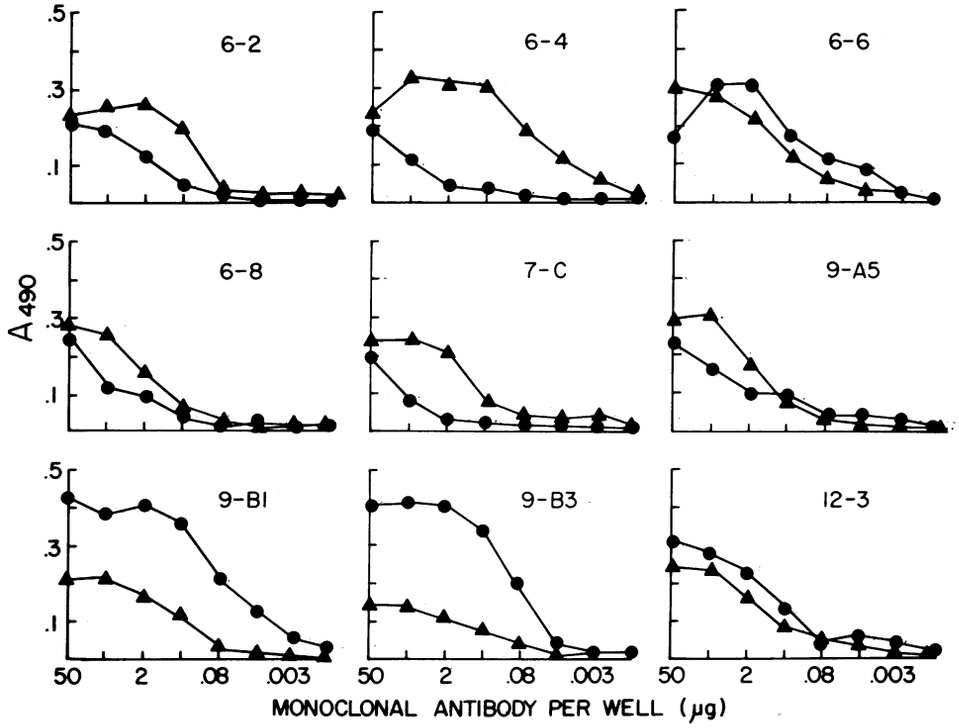

FIG. 1. Monoclonal antibody titration curves in two different ELISAs. Purified antibodies (x axis) were incubated in microtiter wells precoated with 5 μg of purified rat renal Na^+,K^+-ATPase per ml or with glutaraldehyde-fixed primary cultures of 1-day-old hepatocytes (5×10^4 cells plated per well). After incubation with rabbit anti-mouse (IgG and IgM) horseradish peroxidase conjugate, absorbance increases at 490 nm were determined after the addition of H_2O_2 and o-phenylenediamine for either the kidney membrane pump antigen (●) or the hepatocyte ELISA (▲). A_{490} values (y axis) are experimental results minus background (= 0.03 A_{490} unit; determined in the presence of equal amounts of nonimmune mouse IgG).

Binding Properties. Fig. 1 shows titration curves for each purified antibody in each type of ELISA. Table 1 gives antibody concentrations at which half-maximal absorbance was observed (a value proportional to the amount of antibody bound to immobilized antigen). Such concentrations ranged from high titers of 0.5 μg of 6-4 per well (hepatocyte ELISA) to low titers of 100 μg of 7-C per well (antigen ELISA).

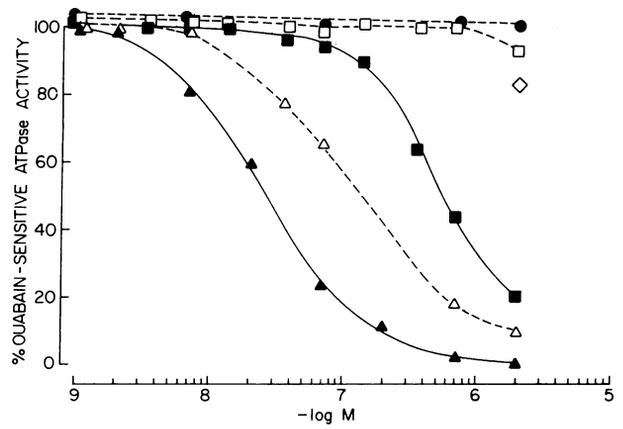

FIG. 2. Effects of monoclonal antibodies on ouabain-sensitive ATPase activity. NADH-coupled enzyme assays were used to quantitate inhibition of ouabain-sensitive ATPase activity. To 25 μg of purified rat renal Na^+,K^+-ATPase, monoclonal antibodies 9-A5 (▲——▲), 9-B1 (■——■), 6-6 (□---□), or R-4 (●---●) were added (at the concentrations given on the x axis). Enzyme activity was determined in reaction mixtures containing 25 mM imidazole (pH 7.5), 100 mM NaCl, 20 mM KCl, and 3 mM $MgCl_2$ after 90 min at 25°C. The P_i-release assay was used to determine enzyme activity in the presence of 9-A5 (△---△). After preincubation and centrifugation of 9-A5 with rabbit anti-mouse IgG, reaction mixture supernatants were tested (◇). Each point is the average of two to five separate determinations (SD ± 10%). Maximal ouabain-sensitive ATPase activity (100%; y axis) was 11.0 μmol of ATP hydrolyzed per mg·min.

Anticatalytic Properties. The ability of each antibody to inhibit enzyme activity was studied in two different ways by using (*i*) luciferase-linked Na^+-ATPase and (*ii*) standard V_{max} Na^+,K^+-ATPase assays.

Five antibodies (6-6, 6-8, 7-C, 9-A5, and 9-B1) inhibited Na^+-ATPase activity (Table 1). Two of them (9-A5 and 9-B1) fully inhibited V_{max} activity (Fig. 2) with K_i (apparent) values of 30 nM and 600 nM, respectively. Hill coefficients for inhibition were ≈1.1. Four other antibodies (6-2, 6-4, 9-B3, and 12-3), including R-4 (a monoclonal antibody specific for rat liver alcohol dehydrogenase) (unpublished data), were inactive. Under these conditions, no apparent correlations were found between anticatalytic and ELISA binding properties (Fig. 1).

Several observations exclude artifactual causes of these anticatalytic effects. For example, enzyme inhibition was due to purified antibody and not to undetectable contaminant molecules because inhibitory effects of 9-A5 were abolished after precipitation of antibody by Sepharose-linked rabbit anti-mouse

Table 2. Inhibition of ATPase activity in crude rat liver membranes by mouse monoclonal antibodies

Addition	Concentration	% control
Ouabain	1 mM	75
Monoclonal antibody 9-A5	1 μM	75
Monoclonal antibody 9-B1	1 μM	54

NADH-coupled enzyme assays were performed and measurements (40 μg of enzyme proteins per point) were made in triplicate. Standard deviations ranged ≈7%. Maximal ATPase activity (100%) was 0.4 μmol of ATP hydrolyzed per mg·min.

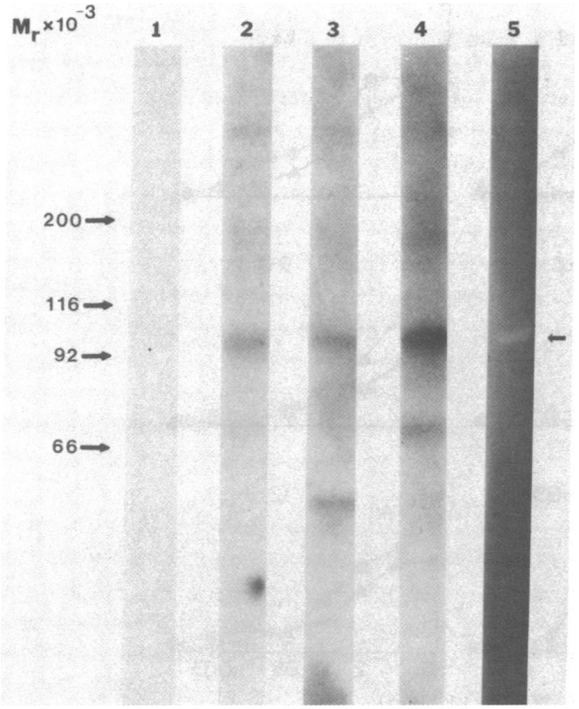

FIG. 3. Autoradiographs of immunoblots of ^{125}I-labeled monoclonal antibodies to purified rat Na^+,K^+-ATPase preparations. Purified enzyme preparations were subjected to $NaDodSO_4$/polyacrylamide gel electrophoresis and were transferred to nitrocellulose paper strips. ^{125}I-labeled antibodies were incubated with the strips for 2 hr at 4°C and washed exhaustively. Lanes 1–4 were incubated with R-4, 6-4, 9-A5, and 9-B1, respectively. Lane 5 is the fluorescent image of the FITC-labeled α subunit of the Na^+,K^+-ATPase. Known protein M_r marker positions, determined from stained gel tracks (not shown), are given at the extreme left (arrows).

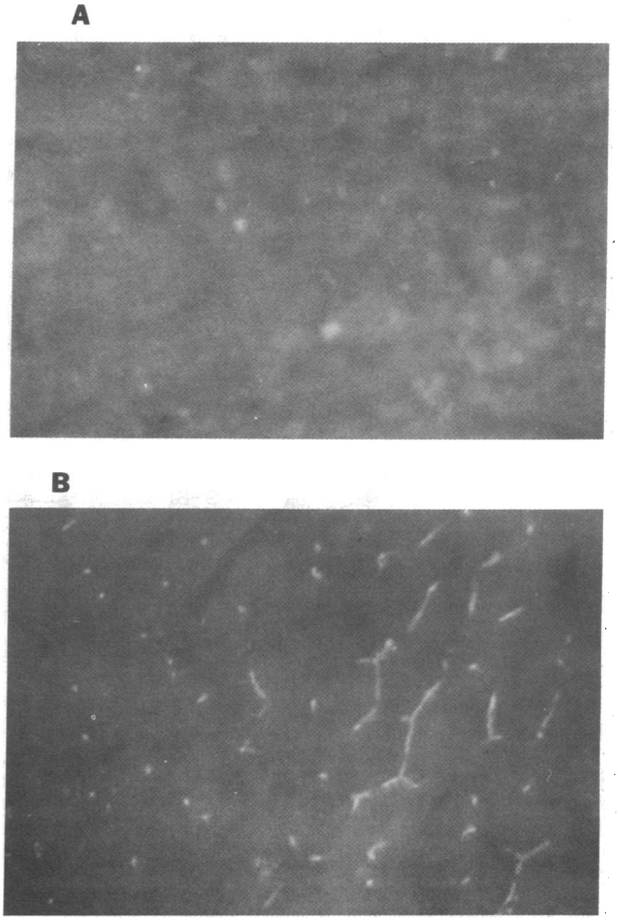

FIG. 4. Immunofluorescent localization of monoclonal antibody 9-B1 binding sites in rat liver tissue. (*A*) Control fluorescence of 20-μm rat liver section after incubation with nonimmune mouse serum, followed by TRITC-labeled rabbit anti-mouse IgG. (*B*) Experimental fluorescence in a serial section after incubation with 100 μg of 9-B1 per ml, followed by TRITC-labeled secondary antibody. (Relative magnification $\approx \times 500$.)

Ig (Fig. 2). Enzyme assay artifacts also are unlikely, for when an alternative ATPase assay was used (measuring P_i release), 9-A5 again fully inhibited Na^+,K^+-ATPase activity, although the K_i (apparent) was increased slightly (Fig. 2). Lastly, indirect perturbations of membrane structure could not account for inhibition because both 9-A5 and 9-B1 retained equivalent inhibitory effects in $C_{12}E_8$-solubilized preparations of kidney Na^+,K^+-ATPase (not shown).

To see if anticatalytic effects were tissue-specific, 9-A5 and 9-B1 were incubated individually with crude rat liver membranes (Table 2). Under these conditions, ATPase activity was inhibited 25% and 46% by 9-A5 and 9-B1, respectively, and 25% by 1 mM ouabain. Reasons why 9-B1 inhibited liver ATPase activity more effectively than ouabain are as yet unknown.

Specificity. Fig. 3 shows autoradiographs of immunoblots containing transferred pump proteins after incubations with ^{125}I-labeled antibodies R-4, 6-4, 9-A5, and 9-B1. Fig. 3 also shows fluorescent detection on $NaDodSO_4$ gels of FITC-labeled Na^+,K^+-ATPase α subunits ($M_r \approx 94{,}000$) blotted under identical conditions (fluorescent labeling of this band was abolished when enzyme reactions with FITC were performed in the presence of 1 mM ATP prior to $NaDodSO_4$/polyacrylamide gel electrophoresis). ^{125}I-Labeled 6-4, 9-A5, and 9-B1 all bound predominantly to transferred proteins that comigrated with Na^+,K^+-ATPase α subunits. Similar results were obtained with 6-6 and 6-8 (not shown). In contrast, ^{125}I-labeled R-4 showed no detectable binding (Fig. 3). Specific binding was lost in the presence of 1,000-fold excess unlabeled specific antibody (not shown). Densitometric scanning under white light of each experimental lane revealed, in each case, a major absorbance peak associated with a 94,000 M_r band (70–80% of the total). Although diffuse minor bands ($\leq$25% of the total absorbance) were seen [$M_r \geq 180{,}000$ (for all three antibodies); $M_r \approx 50{,}000$ (for 9-A5); and $M_r \approx 70{,}000$ (for 9-B1)], antibody binding to them varied and depended upon enzyme isolation conditions and treatments that degrade Na^+,K^+-ATPase (e.g., boiling).

Tissue Localization Properties. Fig. 4 shows the localization of 9-B1 by indirect immunofluorescence to tissue sites in rat liver slices fixed under conditions that preserve membrane glycoprotein structure. After incubation with 9-B1 (primary IgG) and TRITC-labeled goat anti-mouse antibody (secondary IgG), intense fluorescent polygonal arrays and punctate patches were seen (*B*). When nonimmune mouse sera (or R-4) were used as primary antibodies, only nonspecific fluorescence was seen (*A*). Immunofluorescent patterns obtained with 6-4 and 9-A5 were virtually identical with 9-B1. In addition, preincubation of primary antibodies with partially purified rat Na^+,K^+-ATPase prior to localization decreased specific fluorescence to background levels (not shown).

DISCUSSION

Nine distinct monoclonal antibodies have been prepared to purified rat renal Na^+,K^+-ATPase preparations. This conclusion

is based upon a unique profile for each antibody regarding its properties, such as subunit M_r, heavy-chain subclass, and ability to bind to immobilized antigens in different ELISAs or to inhibit catalytic activity of the sodium pump. This latter property, in particular, is observed with five antibodies, two of which (9-A5 and 9-B1) fully inhibit ouabain-sensitive V_{max} activity in both kidney and liver membrane preparations. Because these inhibitory antibodies (and 6-4) bind to epitopes on Na^+,K^+-ATPase α subunits (as judged by immunoblots) and to hepatocyte bile canalicular membrane domains (as judged by immunofluorescence), the antibodies appear to recognize native conformations of rat membrane sodium pumps in different tissues.

Findings of full inhibition of ouabain-sensitive V_{max} activity with 9-A5 and 9-B1 are of considerable interest because inhibition of V_{max} activity with polyclonal pump antisera has rarely been achieved (27, 28). In the few cases in which V_{max} activity was inhibited with polyclonal antisera, large amounts of antiserum (milligram) were required to inhibit microgram quantities of enzyme (28). In contrast, the anticatalytic effects of 9-A5 and 9-B1 occur with half-maximal inhibition of Na^+,K^+-ATPase activity at 1:1 ratios of antibody (9-A5) to enzyme—the most potent reported thus far for antibody to the Na^+ pump. However, whether enzyme-inhibitory effects of 9-A5 (or 9-B1) are due to competitive binding at active sites on α subunits or to inhibition of conformational transitions is unknown.

Because the α subunit of the Na^+,K^+-ATPase binds all known substrates and performs all catalytic functions (29), it would appear that the two V_{max} inhibitory antibodies (9-A5 and 9-B1) block enzyme activity by binding to different α-subunit epitopes. Minor bands of antibody seen on immunoblots at $\geq$180,000 M_r (for all three antibodies) could represent binding to pump oligomers (α_2, $\alpha_2\beta_2$) or different proteins with identical epitopes. The latter possibility seems unlikely, because the probability of three independently derived antibodies binding similarly to two foreign proteins is remote ($<<0.015$) and because other possibly related epitopes on other membrane ATPases—e.g., the Ca^{2+}/Mg^{2+} (30) or H^+/K^+ pump (31)—are found on proteins of 138,000 M_r and 100,000 M_r, respectively. Minor bands seen ($M_r \leq$70,000) probably represent α-subunit degradation products, not binding to the Na^+ pump β subunit ($M_r \approx$ 50,000), because the M_r values of these lower bands vary with each enzyme preparation and treatment.

With respect to those antibodies that inhibited ouabain-sensitive Na^+-ATPase activity, three (6-6, 6-8, and 7-C) had no effect on ouabain-sensitive V_{max} activity. Either they selectively inhibit Na^+-dependent partial reactions of the pump, as reported for polyclonal antisera (15), or they might compete for ATP binding that is masked under V_{max} conditions.

The fluorescent pattern of 9-B1 liver tissue binding sites—polygonal arrays and punctate patches—corresponds to the distribution of alkaline phosphatase, a histochemical marker for bile canalicular membranes (32). The observed pattern also is strikingly similar to bile canalicular staining by fluorescein in living hepatocytes in primary culture (unpublished data). Polygonal arrays probably reflect transverse sections through bile canalicular membrane networks, whereas punctate patches probably arise from sagittal cross sections. Fixation and embedding artifacts cannot account for these observations because formaldehyde-fixed frozen liver sections, 2- to 5-μm thick, gave similar staining patterns with 9B1 (unpublished data). Similar results with 6-4 and 9-A5 further support localization of antibody binding sites to bile canalicular membrane domains (not shown). Although these results do not exclude possibilities that antibody binding sites are present at lower concentrations or as cryptic structures elsewhere in the liver, the findings suggest, but do not prove, that most hepatocyte Na^+ pumps exist in canalicular membranes and not at basolateral and sinusoidal faces (33).†

† After this paper was submitted, we learned of work (34) reporting isolation and partial characterization of monoclonal antibodies to sheep Na^+,K^+-ATPase preparations.

We thank J. Hubert, M. Ellisman, H. Skelly, and G. Fortes for comments, K. Miyai and M. Schumacher for help with immunofluorescence, and S. Dutky for typing. This work was supported by grants from the U.S. Public Health Service (AM28215 and AM28392) and by a predoctoral traineeship to D.B.S. (GM 07752).

1. Koch, K. S. & Leffert, H. L. (1979) *Cell* **18**, 153–163.
2. Leffert, H. L. (1982) in *Ions, Cell Proliferation and Cancer*, eds. Boynton, A., McKeehan, W. L. & Whitfield, J. F. (Academic, New York), pp. 93–102.
3. Leffert, H. L. & Koch, K. S. (1982) in *Ions, Cell Proliferation and Cancer*, eds. Boynton, A., McKeehan, W. L. & Whitfield, J. F. (Academic, New York), pp. 103–130.
4. Rozengurt, E. & Mendoza, S. (1980) *Ann. N.Y. Acad. Sci.* **339**, 175–190.
5. Mummery, C. L., Boonstra, J., Van der Saag, P. T. & de Laat, S. W. (1982) *J. Cell. Physiol.* **112**, 27–34.
6. Baker, P. F. & Willis, J. S. (1972) *J. Physiol. (London)* **224**, 441–462.
7. Leffert, H. L., Koch, K. S., Fehlmann, M., Heiser, W., Lad, P. J. & Skelly, H. (1982) *Biochem. Biophys. Res. Commun.* **108**, 738–745.
8. Lubin, M., Cahn, F. & Coutermarsh, B. A. (1982) *J. Cell. Physiol.* **113**, 247–251.
9. Leffert, H. L., Koch, K. S., Schenk, D. B., Shapiro, P., Skelly, H. & Schumacher, M. (1983) *Electrochem. Soc. Ext. Abstr.* **83**, 988–989.
10. Jörgensen, D. L. (1974) *Biochim. Biophys. Acta* **356**, 36–52.
11. Schwartz, A., Allen, J. C. & Harigaya, S. (1969) *J. Pharmacol. Exp. Ther.* **168**, 31–41.
12. Neville, D. (1964) *Biochim. Biophys. Acta* **154**, 540–552.
13. Engvall, E. (1980) *Methods Enzymol.* **70**, 365–387.
14. Köhler, G. & Milstein, C. (1975) *Nature (London)* **256**, 485–496.
15. Schenk, D. B., Grosse, R., Ellisman, M. H., Bradshaw, V. & Leffert, H. L. (1982) *Anal. Biochem.* **125**, 189–196.
16. Galfré, G. & Milstein, C. (1981) *Methods Enzymol.* **73**, 3–46.
17. Kyte, J. (1971) *J. Biol. Chem.* **246**, 4157–4165.
18. Craig, W. S. (1982) *Biochemistry* **21**, 2667–2674.
19. Lowry, O. H., Rosebrough, N. J., Farr, A. L. & Randall, R. J. (1951) *J. Biol. Chem.* **193**, 265–275.
20. Mancini, G., Carbonara, A. O. & Heremans, J. K. (1965) *Immunochemistry* **2**, 235–243.
21. Carilli, C. T., Farley, R. A., Perlman, D. M. & Cantley, L. C. (1982) *J. Biol. Chem.* **257**, 5601–5606.
22. Burnette, N. (1981) *Anal. Biochem.* **112**, 195–203.
23. Trowbridge, I. S., Ralph, P. & Bevan, M. J. (1975) *Proc. Natl. Acad. Sci. USA* **72**, 157–161.
24. Laemmli, U. K. (1970) *Nature (London)* **227**, 680–685.
25. Morrissey, J. H. (1981) *Anal. Biochem.* **117**, 307–310.
26. McLean, I. W. & Nakane, P. K. (1974) *J. Histochem. Cytochem.* **22**, 1077–1083.
27. Rhee, H. M. & Hokin, L. E. (1979) *Biochem. Biophys. Res. Commun.* **558**, 108–112.
28. McCans, J. L., Lindemayer, G. E., Pitts, B. J. R., Ray, M. V., Raynor, B. B., Butler, V. P. & Schwartz, A. (1975) *J. Biol. Chem.* **250**, 7257–7265.
29. Robinson, J. D. & Flashner, M. S. (1979) *Biochim. Biophys. Acta* **549**, 145–176.
30. Graf, A., Verma, A. K., Gorski, J. P., Lopaschuk, G., Niggli, V., Carafoli, E. & Penniston, J. T. (1982) *Biochemistry* **21**, 4511–4516.
31. Sachs, G., Chang, H. H., Rabon, E., Schackman, R., Lewin, M. & Saccomani, G. (1976) *J. Biol. Chem.* **251**, 7690–7698.
32. Low, M. G. & Finean, J. B. (1978) *Biochim. Biophys. Acta* **508**, 565–570.
33. Blitzer, B. L. & Boyer, I. L. (1978) *J. Clin. Invest.* **62**, 1104–1108.
34. Ball, W. J., Schwartz, A. & Lessard, J. L. (1982) *Biochim. Biophys. Acta* **719**, 413–423.